Full-Duplex Amplify-and-Forward Relay System with Direct Link: Performance Analysis and Optimization

Ba Cao Nguyen*, Xuan Nam Tran*, Dinh Tan Tran†, Le The Dung‡,
*Le Quy Don Technical University, Vietnam, Emails: bacao.sqtt@gmail.com, namtx@mta.edu.vn
†Telecommunication University, Vietnam, Email: trdinhtan@gmail.com
‡Ton Duc Thang University, Vietnam, Email: lethedung@tdtu.edu.vn

Abstract

In this paper, we analyze performance of the full-duplex (FD) amplify-and-forward (AF) relay system under various cases of relaying gains and channel state information conditions. Specifically, we consider the case that the FD relay node uses either fixed or variable gain for relaying under perfect and imperfect channel state information (CSI). For the case of imperfect CSI (I-CSI), we derive the exact expressions for the outage probability (OP), throughput, and symbol error probability (SEP) of the considered system. For the case of perfect CSI (P-CSI), we can provide approximate expressions of OP, throughput, SEP, and ergodic capacity. In the case of P-CSI we also propose an effective power allocation scheme for the FD relay node in order to reduce the impact of residual self-interference (RSI). Both analytical and simulation results show a significant impact of RSI on the system performance. In particular, when RSI is small the variable-gain relaying can help to achieve better performance than the fixed gain. However, if RSI becomes large the two relaying schemes provide a similar performance. In this case, using the proposed optimal power allocation scheme can improve the system performance, especially for the case with weak direct link.

Index Terms

Full-duplex, residual self interference, self-interference cancellation, amplify-and-forward, ergodic capacity, outage probability, symbol error probability.

I. Introduction

Nowadays, there is a continuously rising demand for high speed wireless broadband and reliable networks for both commercial and mission-critical communications. While the wireless mobile services can rely on the

Part of the paper was published at the 2nd International Conference on Recent Advances in Signal Processing, Telecommunications and Computing (SigTelCom2018), Ho Chi Minh, Vietnam [1].

Corresponding author, Le The Dung is with Divison of Computational Physics, Institute for Computational Science, Ton Duc Thang University, Ho Chi Minh City, Vietnam; Faculty of Electrical and Electronics Engineering, Ton Duc Thang University, Ho Chi Minh City, Vietnam, lethedung@tdtu.edu.vn

existing communication infrastructure provided by the telco and internet service providers, the mission-critical communication often requires more bandwidth to support disaster and emergency situations. In order to meet this requirement, a wireless system that can provide bandwidth-efficient services for data/video transmission is vitally needed. Various physical-layer transmission solutions such as massive multiple-input multiple-output (MIMO), spatial modulation, non-orthogonal multiple access (NOMA), in-band full-duplex (IBFD) or full-duplex (FD) were proposed to improve the spectrum efficiency [2]–[7].

With the advantage of doubling the spectral efficiency, the FD communication is considered a potential solution for the mission-critical voice and data communication systems [8]–[10]. However, the residual self-interference (RSI) due to imperfect self-interference cancellation (SIC) in the FD mode has a strong impact on the system performance [11]–[14]. It is the RSI that prevents the FD communication from the practical deployment [3], [15]–[17]. With the recent advancements in antenna design, analog and digital signal processing, the FD devices can suppress the self-interference up to 110 dB [18]–[21], making the FD communication become more feasible. Meanwhile, due to the benefits and wide deployments of the relay networks [22], the integration of the FD mode to the cooperative communication systems can provide promising improvements in signal coverage, transmission reliability, and spectral efficiency. Therefore, large efforts were paid to study the potential of the FD relay systems in the literature [23]–[27].

Performance of the FD relay systems under various conditions were thoroughly studied in [1], [15], [28]–[35]. Using theoretical analysis, the outage probability (OP) performance and the end-to-end capacity were investigated [28], [29], [36], [37]. In [28], the authors considered an amplify-and-forward (AF) FD relay system which uses the maximal-ratio combining (MRC) to combine received signals from the direct and relaying links. Exact and approximate expressions of OP for the case of variable-gain relaying were derived but not in the closed-form. Meanwhile, the work in [38] investigated a similar system with both fixed and variable-gain relaying and found that the system can achieve the same diversity order for both cases. Assuming the availability of the direct link from the source to the destination while treating the RSI as a noise component, the paper [29] analyzed the OP performance of the AF FD relay system. However, the closed-form expression for OP of this system was not provided. In order to balance the spectral efficiency with the system performance, the work [36] proposed a hybrid FD/HD relay which can combine the opportunistic duplex mode selection and transmit power adaptation. At the destination, the received signal via the direct link is considered as noise or useful signal according to the FD or HD mode at the relay node. It was shown that the hybrid FD/HD relay is highly efficient in the case of imperfect SIC. With the same assumption of having the direct link, [37] analyzed the outage performance of the AF FD relay system.

Recent researches in the literature also considered the FD relay communication systems using NOMA. In [39] and [40], the authors considered the case that the near user acts as the FD relay to forward the signal from the basestation to the far user. The exact expressions for the OP were successfully derived for both the users. In [33], the authors investigated an AF FD cooperative NOMA system with approximated relaying gain and derived its OP and ergodic capacity. The closed-form expressions for OP was not obtained in this paper. In [35], the outage performance of a downlink FD cooperative NOMA system using energy harvesting (EH) at the FDR was analyzed. The exact expressions of the OP for both the near and far users over the Nakagami-m fading channel was provided. However, these expressions still contain integrals but not in the closed-form.

Although the performance of the AF FD relay systems was analyzed in various works, the full understanding on it for the case there exists the direct link is still limited, possibly due to complicated mathematical derivations. In the previous works, the direct link was either neglected or considered only for the case of the HD relays. Although some works considered the case with the direct link [28], [33], [35], [39], [40], they did not provide the closed-form expression for OP. The expressions for the achievable capacity and symbol error probability (SEP) were also overlooked. Considering the use of different relaying gains for the FD relay, the works [28], [33] considered only the case that perfect CSI is available, i.e. the variable-gain relaying is used, at the relay node. Given partial CSI, the relay should use a fixed gain but the analysis for this case were not reported yet. In order to address these problems, in this paper we conduct a detailed performance analysis of the AF FD relay system with the direct link and using both fixed and variable-gain relaying. Different from previous works, we can obtain the closed-form expression for OP in the case of variable gain relaying by using approximation method. In the case of fixed gain relaying, to avoid large approximation error we resort to the Gaussian-Chebyshev quadrature method to obtain the exact closed-form OP expression. Besides the OP, we also derive other performance measures such as the system throughput, ergodic capacity, and SEP of the considered system. In order to deal with the RSI impact, we propose an effective optimal power allocation scheme for performance improvement. In summary, the contributions of this paper can be stated as follows:

- We derive the exact closed-form expression for the OP of the FD AF relay system with the direct link for the case with fixed-gain and variable-gain under the case of partial CSI (P-CSI) and full CSI (F-CSI) at the relay node. In the case of P-CSI, we can derive the exact closed-form expression for OP while in the other case using the approximation method, we can convert the integral-form to an exact closed-form expression for the OP. Based on this expression, we can obtain the closed-form expressions for the system throughput, SEP and ergodic capacity of the FD AF relay system.
- We evaluate the system performances in terms of OP, throughput, SEP and ergodic capacity for the case of imperfect SIC, fixed and varied RSI. The impacts of the RSI, the channel gain of direct link, the transmission power of the FD relay node are also investigated.
- We propose an optimal power allocation scheme to reduce the impact of RSI in the high signal-to-noise ratio (SNR) regime. Using the proposed power allocation scheme, we can enhance the system performance significantly.

The rest of this paper is organized as follows. Section II describes the system model. Performances of the system in terms of OP, throughput, SEP and ergodic capacity are analyzed in Section III. Section IV presents the optimal power allocation scheme. Numerical results and discussions are given in Section V. Finally, conclusions are drawn in Section VI.

II. System Model

The system model of the AF FD relay system with the direct link under consideration is illustrated in Fig. 1. A source node S transmits its signal to a destination node D via two links: (i) the relaying link with the help of a relay node R, and (ii) the direct link from S to D (hereinafter referred to as the direct link). In this model, S and D are assumed to have one antenna and operate in the HD mode while R has two antennas to support the FD mode, one for reception and one for transmission simultaneously. Note that the use of two separate antennas instead of a shared-antenna by R allows for better isolation.

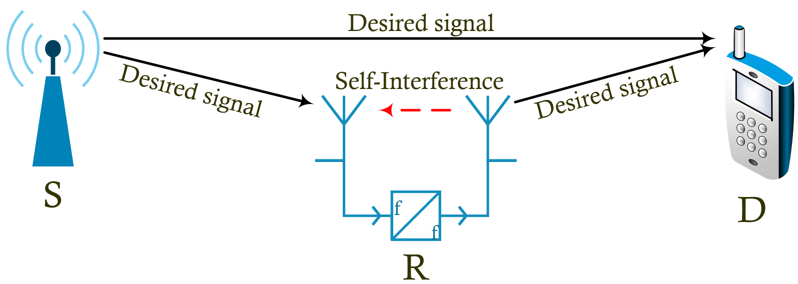

Fig. 1. System model of the AF FD relay system with direct link.

At time slot t, the received signal at the relay node is given by

$$y_{\mathrm{R}} = h_{\mathrm{SR}} x_{\mathrm{S}} + \tilde{h}_{\mathrm{RR}} x_{\mathrm{R}} + z_{\mathrm{R}}, \tag{1}$$

where h_{SR} and $\tilde{h}_{\mathrm{RR}}$ are respectively the fading coefficients of the channels from S to R and from the transmitting antenna to the receiving antenna of R; x_{S} and x_{R} are the transmitted signals from S and R, respectively; z_{R} is the Additive White Gaussian Noise (AWGN) with zero-mean and variance σ_{R}^2, i.e. $z_{\mathrm{R}} \sim \mathcal{CN}(0, \sigma_{\mathrm{R}}^2)$. It is assumed that the relay R can apply all available SIC techniques in the propagation, analog and digital domain for the best-effort self-interference suppression. However, a certain level of the RSI still exists due to imperfect SIC, which impacts the system performance. Under this assumption, the RSI at the FD relay node, denoted by I_{R}, can be modeled as a complex Gaussian-distributed random variable with zero mean and variance σ_{RSI}^2. The RSI variance was analyzed in [28], [41]–[44] and given by $\sigma_{\mathrm{RSI}}^2 = \tilde{\Omega}_{\mathrm{R}} P_{\mathrm{R}}$, where $\tilde{\Omega}_{\mathrm{R}}$ represents the SIC capability of the FD relay node.

The received signal at R after SIC is then given by

$$y_{\mathrm{R}} = h_{\mathrm{SR}} x_{\mathrm{S}} + I_{\mathrm{R}} + z_{\mathrm{R}}. \tag{2}$$

Next, using the AF protocol, the relay R amplifies the received signal before forwarding it to the D, i.e.

$$x_{\mathrm{R}} = G y_{\mathrm{R}}, \tag{3}$$

where G is the relaying gain. The value of the relaying gain is adjusted so that the transmit power of R equals P_{R}, i.e.

$$\mathbb{E}\left\{|x_{\mathrm{R}}|^2\right\} = G^2 \mathbb{E}\left\{|y_{\mathrm{R}}|^2\right\} = P_{\mathrm{R}}, \tag{4}$$

where $\mathbb{E}\{\cdot\}$ represents the expectation operator. In the case of P-CSI, i.e. R has perfect knowledge of the fading coefficient $h_{\rm SR}$, it uses a variable gain $G_{\rm v}$ which can be changed according to the fading state. Otherwise, it uses a fixed gain $G_{\rm f}$. These fixed and variable gains are calculated given as follows

$$G_{\rm f} \triangleq \sqrt{\frac{P_{\rm R}}{\Omega_1 P_{\rm S} + \sigma_{\rm RSI}^2 + \sigma_{\rm R}^2}}, \tag{5}$$

$$G_{\rm v} \triangleq \sqrt{\frac{P_{\rm R}}{\rho_1 P_{\rm S} + \sigma_{\rm RSI}^2 + \sigma_{\rm R}^2}}, \tag{6}$$

where $\rho_1 = |h_{\rm SR}|^2$ and $\Omega_1 = \mathbb{E}\{\rho_1\}$ are, respectively, the instantaneous and average channel gains of the S–R link; $P_{\rm S}$ is the average transmit power of S.

The received signal at the destination node D can be expressed as

$$y_{\rm D} = h_{\rm RD} x_{\rm R} + h_{\rm SD} x_{\rm S} + z_{\rm D}, \tag{7}$$

where $h_{\rm RD}$ and $h_{\rm SD}$ are the fading coefficients of the R–D and S–D link, respectively; $z_{\rm D} \sim C\mathcal{N}(0, \sigma_{\rm D}^2)$ is the AWGN at the destination node.

Based on equations (2), (3) and (7), the received signal at D can be given by

$$y_{\rm D} = h_{\rm RD} G \Big[h_{\rm SR} x_{\rm S} + I_{\rm R} + z_{\rm R}\Big] + h_{\rm SD} x_{\rm S} + z_{\rm D}. \tag{8}$$

It is also noted that since the relay node R needs to process the received signal before forwarding, the destination node may receive the signal via the direct link later than that from the relaying link. To combine these signals, similar to [33], [45] we assume that D can fully resolve them using some suitable processing method such as the ideal Rake one [28]. Then D can appropriately co-phase and merge these two signals using the MRC technique. Using (8), the end-to-end signal-to-interference-plus-noise ratio (SINR) of the considered system is expressed as

$$\gamma = \gamma_{\rm SD} + \gamma_{\rm SRD}, \tag{9}$$

where $\gamma_{\rm SD}$ and $\gamma_{\rm SRD}$ are the SINR of S–D and S–R–D link, respectively; $\gamma_{\rm SD}$ is given by

$$\gamma_{\rm SD} = \frac{|h_{\rm SD}|^2 P_{\rm S}}{\sigma_{\rm D}^2} = \frac{\rho_3 P_{\rm S}}{\sigma_{\rm D}^2}, \tag{10}$$

while $\gamma_{\rm SRD}$ is calculated for the two cases corresponding to $G_{\rm f}$ and $G_{\rm v}$ as follows

$$\begin{aligned} \gamma_{\rm SRD}^{\rm f} &= \frac{|h_{\rm SR}|^2 |h_{\rm RD}|^2 P_{\rm S}}{|h_{\rm RD}|^2 (\sigma_{\rm RSI}^2 + \sigma_{\rm R}^2) + \sigma_{\rm D}^2/(G_{\rm f})^2} \\ &= \frac{\rho_1 \rho_2 P_{\rm S}}{\rho_2 (\sigma_{\rm RSI}^2 + \sigma_{\rm R}^2) + \sigma_{\rm D}^2/(G_{\rm f})^2}, \end{aligned} \tag{11}$$

$$\gamma_{\rm SRD}^{\rm v} = \frac{\rho_1 \rho_2 P_{\rm S} P_{\rm R}}{(\rho_2 P_{\rm R} + \sigma_{\rm D}^2)(\sigma_{\rm RSI}^2 + \sigma_{\rm R}^2) + \rho_1 P_{\rm S} \sigma_{\rm D}^2}, \tag{12}$$

where $\rho_1 = |h_{\rm SR}|^2$; $\rho_2 = |h_{\rm RD}|^2$; $\rho_3 = |h_{\rm SD}|^2$.

Note that the fixed gain in (5) can be obtained from the variable gain by setting $\rho_1 = \Omega_1$ in (6). However, the SINR of the case with fixed gain relaying cannot be obtained from the SINR of variable gain relaying by using the same way. This is because when we set $\rho_1 = \Omega_1$ in (12) the random channel gain of the S– R link becomes 1. Thus, we cannot derive (11) from (12). As a result, both OP and SEP, as well as other performance parameters in the system with fixed gain relaying cannot be derived from the expressions of the case with variable gain relaying.

It is also noted that when the instantaneous channel gains follow Rayleigh fading distribution, the cumulative distribution function (CDF), denoted by $F(x)$, and the probability density function (PDF), denoted by $f(x)$, of ρ_i, $i = 1, 2, 3$, are given, respectively, by

$$F_{\rho_i}(x) = 1 - e^{-\frac{x}{\Omega_i}}, x \geq 0, \tag{13}$$

$$f_{\rho_i}(x) = \frac{1}{\Omega_i} \exp\left(-\frac{x}{\Omega_i}\right), x \geq 0, \tag{14}$$

where $\Omega_i = \mathbb{E}\{\rho_i\}$.

III. Performance Analysis

Based on the signal equations in the previous section, in this section we analyze the system performance and derive the closed-form expressions of OP, throughput, SEP, and ergodic capacity for both the cases with fixed gain relaying and variable gain relaying.

A. Outage Probability

The OP of the considered FD relay system is defined as the probability that the achievable rate falls below a target data transmission rate. Let $\mathcal{R}$ (bit/s/Hz) and C be the target and instantaneous rate of the system, respectively. Then, the OP of the FD relay system is expressed as

$$P_{\text{out}} = \Pr\{C < \mathcal{R}\}, \tag{15}$$

where $C = \log_2(1 + \gamma)$; γ is the end-to-end SINR of the system. Consequently, we have

$$\log_2(1 + \gamma) < \mathcal{R}, \tag{16}$$

which leads to

$$\gamma < 2^{\mathcal{R}} - 1. \tag{17}$$

Let $x = 2^{\mathcal{R}} - 1$ be the threshold, we can calculate the OP of the considered system using the following expression

$$P_{\text{out}} = \Pr\{\gamma < x\}. \tag{18}$$

The OP of the system in both the cases of fixed and variable gain relaying is then given by Theorem 1.

Theorem 1: The OP expressions of the considered system in the case of fixed gain, denoted by $P_{\text{out}}^{\text{f}}$, and variable gain relaying, denoted by $P_{\text{out}}^{\text{v}}$, are calculated, respectively, as follows

$$\begin{aligned} P_{\text{out}}^{\text{f}} &= \Pr\{\gamma_{\text{f}} < x\} = \Pr\{\gamma_{\text{SD}} + \gamma_{\text{SRD}}^{\text{f}} < x\} \\ &= 1 - \exp(-b_{\text{f}}x) - \frac{b_{\text{f}}x}{2}\exp(-b_{\text{f}}x)\sum_{n=1}^{N}\frac{\pi}{N}\sqrt{1-\phi_n^2}G(u), \end{aligned} \tag{19}$$

$$P_{\text{out}}^{\text{v}} = \Pr\{\gamma_{\text{v}} < x\} = \Pr\{\gamma_{\text{SD}} + \gamma_{\text{SRD}}^{\text{v}} < x\}$$
$$\approx \begin{cases} 1 - \frac{a_{\text{v}} \exp(-b_{\text{v}} x)}{a_{\text{v}} - b_{\text{v}}} - \frac{b_{\text{v}} \exp(-a_{\text{v}} x)}{b_{\text{v}} - a_{\text{v}}}, & a_{\text{v}} \neq b_{\text{v}}, \\ 1 - b_{\text{v}} x \exp(-a_{\text{v}} x) - \exp(-b_{\text{v}} x), & a_{\text{v}} = b_{\text{v}}, \end{cases} \tag{20}$$

where $K_1(\cdot)$ denotes the first-order modified Bessel function of the second kind [46], N is the complexity-accuracy trade-off parameter, $\phi_n = \cos\left(\frac{(2n-1)\pi}{2N}\right)$, $u = \frac{x}{2}(\phi_n + 1)$, $a_{\text{f}} = \frac{\sigma_{\text{RSI}}^2 + \sigma_{\text{R}}^2}{\Omega_1 P_{\text{S}}} - \frac{\sigma_{\text{D}}^2}{\Omega_3 P_{\text{S}}}$, $b_{\text{f}} = \frac{\sigma_{\text{D}}^2}{\Omega_3 P_{\text{S}}}$, $a_{\text{v}} = \frac{\sigma_{\text{RSI}}^2 + \sigma_{\text{R}}^2}{\Omega_1 P_{\text{S}}} + \frac{\sigma_{\text{D}}^2}{\Omega_2 P_{\text{R}}}$, $b_{\text{v}} = \frac{\sigma_{\text{D}}^2}{\Omega_3 P_{\text{S}}}$,

$$G(u) = 2\exp(-a_{\text{f}} u) \sqrt{\frac{\sigma_{\text{D}}^2 u}{\Omega_1 \Omega_2 P_{\text{S}} G_{\text{f}}^2}} K_1 \left(2\sqrt{\frac{\sigma_{\text{D}}^2 u}{\Omega_1 \Omega_2 P_{\text{S}} G_{\text{f}}^2}} \right). \tag{21}$$

Proof: In the case of fixed gain G_{f}, using [46, Eq. 3.324.1] together with the partial integration and the Gaussian-Chebyshev quadrature method [47], we can obtain OP of the AF FD relay system in (19). In the case of variable gain relaying, combining [46, Eq. 3.324.1] with the approximation $K_1(X) \approx \frac{1}{X}$ when $X \ll 1$ [47], the system OP is given in (20). After some algebraic manipulations, we can transform the integral-form of OP from (43) to the closed-form in (20). For detailed derivations, see Appendix A.

B. System Throughput

For wireless systems, the system throughput is another important performance metric that needs to be evaluated. The system throughput, which is denoted by $\mathcal{T}$, is defined as

$$\mathcal{T}(x) = \mathcal{R}(1 - P_{\text{out}}), \tag{22}$$

where $\mathcal{R}$ is the desired transmission rate (bit/s/Hz); P_{out} is OP of the considered system, which is given respectively in (19) and (20) for the case of fixed and variable gain relaying.

C. Symbol Error Probability

The symbol error probability of the wireless system is computed as follows [48]

$$\text{SEP} = \alpha \mathbb{E}\left\{ Q\left(\sqrt{\beta\gamma}\right) \right\} = \frac{\alpha}{\sqrt{2\pi}} \int_0^\infty F_\gamma\left(\frac{t^2}{\beta}\right) e^{-\frac{t^2}{2}} dt, \tag{23}$$

where α and β are constants and their values are determined through the modulation types, e.g., $\alpha = 1, \beta = 2$ for the binary phase-shift keying (BPSK) modulation [48]; $Q(x) = \frac{1}{\sqrt{2\pi}} \int_x^\infty e^{-t^2/2} dt$ is the Gaussian function, γ is the end-to-end SINR of the considered system, $F_\gamma(x)$ is the CDF of the SINR, which can be replaced by P_{out} of the considered system through the definitions of CDF and outage probability; P_{out} is determined from (19) and (20) for the case of fixed and variable gain relaying, respectively.

Based on (23), after some mathematical calculations, we obtain the SEP of the considered system for the two cases in Theorem 2 presented below.

Theorem 2: The SEPs of the AF FD relay system in the case of fixed and variable gains are determined as follows:

$$\mathrm{SEP}^{\mathrm{f}} = \frac{\alpha\sqrt{\beta}}{2}\left[\frac{1}{\sqrt{\beta}} - \frac{1}{\sqrt{\beta+2b_{\mathrm{f}}}} - \frac{b_{\mathrm{f}}}{2N}\sqrt{\frac{\pi}{2}}\Gamma\left(\frac{5}{2}\right)\Gamma\left(\frac{3}{2}\right)M\right], \tag{24}$$

$$\mathrm{SEP}^{\mathrm{v}} = \begin{cases} \frac{\alpha\sqrt{\beta}}{2}\Big[\frac{1}{\sqrt{\beta}} - \frac{1}{a_{\mathrm{v}}-b_{\mathrm{v}}}\Big(\frac{b_{\mathrm{v}}}{\sqrt{\beta+2a_{\mathrm{v}}}} - \frac{a_{\mathrm{v}}}{\sqrt{\beta+2b_{\mathrm{v}}}}\Big)\Big], & a_{\mathrm{v}} \neq b_{\mathrm{v}}, \\ \frac{\alpha\sqrt{\beta}}{2}\Big(\frac{1}{\sqrt{\beta}} - \frac{1}{\sqrt{\beta+2b_{\mathrm{v}}}} - \frac{b_{\mathrm{v}}}{\sqrt{(\beta+2a_{\mathrm{v}})^3}}\Big), & a_{\mathrm{v}} = b_{\mathrm{v}}, \end{cases} \tag{25}$$

where

$$M = \sum_{n=1}^{N}\sqrt{1-\phi_n^2}\exp\Big(\frac{\chi^2}{2\varphi}\Big)\varphi^{-\frac{3}{2}}W_{-\frac{3}{2},\frac{1}{2}}\Big(\frac{\chi^2}{\varphi}\Big), \tag{26}$$

with

$$\chi = \sqrt{\frac{\sigma_{\mathrm{D}}^2(1+\phi_n)}{2\Omega_1\Omega_2 P_{\mathrm{S}} G_{\mathrm{f}}^2}};\varphi = a_{\mathrm{f}}\frac{1+\phi_n}{2} + b_{\mathrm{f}} + \frac{\beta}{2}; \tag{27}$$

and W is the Whittaker function [46].

Proof: By setting $x = \frac{t^2}{\beta}$, we can rewrite (23) as

$$\mathrm{SEP} = \frac{\alpha\sqrt{\beta}}{2\sqrt{2\pi}}\int_0^{\infty}\frac{e^{-\beta x/2}}{\sqrt{x}}F_{\gamma}(x)dx. \tag{28}$$

To obtain the SEP, we replace $F_{\gamma}(x)$ in (28) by P_{out} in (19) and (20) then use [46, Eq. 3.361.2], [46, Eq. 6.643.3] for the $\mathrm{SEP}^{\mathrm{f}}$ and [46, Eq. 2.321.1], [46, Eq. 3.361.2] for the $\mathrm{SEP}^{\mathrm{v}}$ to have the results in Theorem 2. For detailed proof, see Appendix B.

D. Ergodic Capacity

In this section, we derive the ergodic capacity of the considered system in the case of variable gain at the relay node. For the AF FD relay system, the ergodic capacity is calculated as follows

$$C_{\mathrm{FD}}^{\mathrm{v}} = \mathbb{E}\Big\{\log_2(1+\gamma_{\mathrm{v}})\Big\} = \int_0^{\infty}\log_2(1+\gamma_{\mathrm{v}})f_{\gamma_{\mathrm{v}}}(\gamma)d\gamma, \tag{29}$$

where γ_{v} is the end-to-end SINR of the considered system with variable gain relaying and $f_{\gamma_{\mathrm{v}}}(\gamma)$ is the PDF of γ_{v}. Based on (29), we obtain the ergodic capacity of the considered system in the case of variable gain relaying in Theorem 3.

Theorem 3: The ergodic capacity of the AF FD relay system in the case of variable gain at the relay node is given by

$$C_{\mathrm{FD}}^{\mathrm{v}} = \begin{cases} \frac{1}{\ln 2}\left[\frac{a_{\mathrm{v}}e^{b_{\mathrm{v}}}}{a_{\mathrm{v}}-b_{\mathrm{v}}}E_1(b_{\mathrm{v}}) + \frac{b_{\mathrm{v}}e^{a_{\mathrm{v}}}}{b_{\mathrm{v}}-a_{\mathrm{v}}}E_1(a_{\mathrm{v}})\right], & a_{\mathrm{v}} \neq b_{\mathrm{v}}, \\ \frac{1}{\ln 2}\left[\frac{b_{\mathrm{v}}}{a_{\mathrm{v}}} - b_{\mathrm{v}}e^{a_{\mathrm{v}}}E_1(a_{\mathrm{v}}) + e^{b_{\mathrm{v}}}E_1(b_{\mathrm{v}})\right], & a_{\mathrm{v}} = b_{\mathrm{v}}, \end{cases} \tag{30}$$

where $E_1(\cdot)$ is the exponential integral which is defined in [46] as $E_1(x) = \int\limits_x^{\infty}\frac{e^{-t}}{t}dt$.

Proof: From (29), we can calculate the ergodic capacity after some mathematical manipulations as follows

$$C_{\mathrm{FD}}^{\mathrm{v}} = \frac{1}{\ln 2} \int_{0}^{\infty} \frac{1 - F_{\gamma}(x)}{1+x} dx, \tag{31}$$

Replacing $F_{\gamma}(x)$ in (31) by OP in (20) and using [46, Eq. 3.352.4], we obtain (30).

IV. Optimal Power Allocation for FD Mode

In this section, an optimal power allocation scheme for the case of variable gain at the relay is proposed to minimize the OP and SEP of the considered system by reducing the RSI at FD relay node. As a consequence, the throughput and the ergodic capacity will be maximized. The optimal value of P_{R}, denoted by P_{R}^{*}, is calculated from the transmission power of source node, the average channel gains and the variance of AWGN at destination node.

The optimization problem is expressed as

$$\begin{aligned} &\min P_{\mathrm{out}}^{\mathrm{v}} \\ &s.t \; P_{\mathrm{R}} > 0 \end{aligned} \tag{32}$$

To solve this problem we use the linear programming method. The closed-form optimal power expression at the relay, denoted by P_{R}^{*} , is given by

$$P_{\mathrm{R}}^{*} = \arg \min_{P_{\mathrm{R}}} P_{\mathrm{out}}^{\mathrm{v}}, \tag{33}$$

where $P_{\mathrm{out}}^{\mathrm{v}}$ is given in (20). Then, the optimal power can be achieved by using Algorithm 1 below.

Algorithm 1 Optimal Power Calculation Algorithm

1: Solve $\frac{\partial P_{\mathrm{out}}^{\mathrm{v}}}{\partial P_{\mathrm{R}}} = 0$ to get $P_{\mathrm{R}} = P_0$;

2: **if** $\begin{cases} P_0 > 0 \\ \dfrac{\partial P_{\mathrm{out}}^{\mathrm{v}}}{\partial P_{\mathrm{R}}} < 0 \text{ for } P_{\mathrm{R}} < P_0 \\ \dfrac{\partial P_{\mathrm{out}}^{\mathrm{v}}}{\partial P_{\mathrm{R}}} > 0 \text{ for } P_{\mathrm{R}} > P_0 \end{cases}$ **then**

3: Output optimal power value

$$P_{\mathrm{R}}^{*} = P_0;$$

4: **else**

5: Output optimal power value

$$P_{\mathrm{R}}^{*} = \emptyset;$$

6: **end**

It is noted that in the case $P_{\mathrm{R}}^{*} = \emptyset$, depending on whether $\frac{\partial P_{\mathrm{out}}^{\mathrm{v}}}{\partial P_{\mathrm{R}}}$ is less or greater than 0, we will select an appropriate value of P_{R}. Furthermore, as shown in Algorithm 1, the proposed algorithm requires only a comparison operation of the first derivative to decide the optimal P_R^*. Meanwhile, the first derivative of $P_{\text{out}}^{\text{v}}$ is given in (35) with the exponential term given in (36). The complexity requirement is thus not significant.

Based on Algorithm 1, we have the optimal power value of the transmission power of the FD relay node given by Theorem 4.

Theorem 4: The optimal power value at the FD relay node is given by

$$P_{\text{R}}^* = \sqrt{\frac{\Omega_1 P_{\text{S}} \sigma_{\text{D}}^2}{\Omega_2 \tilde{\Omega}_{\text{R}}}}. \tag{34}$$

Proof: In the case $a_{\text{v}} = b_{\text{v}}$, there is only one value of P_{R} which satisfies this equation. Whereas in the case $a_{\text{v}} \neq b_{\text{v}}$, by using Algorithm 1 and taking the derivative of $P_{\text{out}}^{\text{v}}$ with respect to P_{R}, we have

$$\begin{aligned}\frac{\partial P_{\text{out}}^{\text{v}}}{\partial P_{\text{R}}} &= -\left[\frac{a_{\text{v}}' b_{\text{v}} e^{-a_{\text{v}} x}}{(b_{\text{v}} - a_{\text{v}})^2} - \frac{a_{\text{v}}' b_{\text{v}} x e^{-a_{\text{v}} x}}{(b_{\text{v}} - a_{\text{v}})} - \frac{a_{\text{v}}' b_{\text{v}} e^{-b_{\text{v}} x}}{(a_{\text{v}} - b_{\text{v}})^2}\right] \\ &= \frac{a_{\text{v}}' b_{\text{v}} e^{-a_{\text{v}} x}}{(b_{\text{v}} - a_{\text{v}})^2}\left[-1 + (b_{\text{v}} - a_{\text{v}})x + e^{(a_{\text{v}} - b_{\text{v}})x}\right],\end{aligned} \tag{35}$$

where $a_{\text{v}}' = \frac{\partial a_{\text{v}}}{\partial P_{\text{R}}} = \frac{\tilde{\Omega}_{\text{R}}}{\Omega_1 P_{\text{S}}} - \frac{\sigma_{\text{D}}^2}{\Omega_2 P_{\text{R}}^2}; b_{\text{v}}' = \frac{\partial b_{\text{v}}}{\partial P_{\text{R}}} = 0$. Using the Taylor expansion, we can rewrite the exponent term $e^{(a_{\text{v}} - b_{\text{v}})x}$ as follows

$$\begin{aligned}e^{(a_{\text{v}} - b_{\text{v}})x} &= \sum_{n=0}^{\infty} \frac{[(a_{\text{v}} - b_{\text{v}})x]^n}{n!} \\ &= 1 + (a_{\text{v}} - b_{\text{v}})x + \frac{[(a_{\text{v}} - b_{\text{v}})x]^2}{2!} + \cdots\end{aligned} \tag{36}$$

Replacing (36) into (35), we can find only one critical point as given in (34) because (35) equals to 0 only when $a_{\text{v}}' = 0$.

V. Numerical Results and Discussions

In this section, the system performance of the AF FD relay system is evaluated by using the derived mathematical expressions in previous section. To prove the correctness of theoretical analysis, we also show the Monte-Carlo simulated results versus the numerical ones. In our results, we choose the average channel gains $\Omega_1 = \Omega_2 = 1$ and the noise variances $\sigma_{\text{R}}^2 = \sigma_{\text{D}}^2 = 1$. The complexity-accuracy trade-off parameter $N = 20$. The system performance is examined for different SNRs. Here we define the average SNR as the ratio of the average transmit power (P_{S} and P_{R}) to the noise variances (σ_{R}^2 and σ_{D}^2), i.e. $\text{SNR} = P_{\text{S}}/\sigma_{\text{R}}^2 = P_{\text{R}}/\sigma_{\text{D}}^2$ for the case without optimization. In the case with optimization is used, the average SNR is $\text{SNR} = P_{\text{S}}/\sigma_{\text{R}}^2$. Furthermore, the notations "wi. op" and "wo. op" in Fig. 5 and the following figures denote the cases with and without using optimal power allocation at the relay node, respectively.

Fig. 2 and Fig. 3 depict the OP curves of the considered system versus the average SNR, which were plotted by using (19) for the case with fixed gain (Fig. 2) and (20) for the case with variable gain relaying (Fig. 3). The expected transmission rate which is used to obtain the OP is $\mathcal{R} = 2$ bit/s/Hz, thus $x = 2^{\mathcal{R}} - 1 = 3$. Since the distance from S to D is large, we assume that the average channel gain of the S–D link is $\Omega_3 = 0.1$ which is smaller than $\Omega_1 = \Omega_2 = 1$. Four RSI power levels used for simulations are: $\frac{\sigma_{\text{RSI}}^2}{\sigma_{\text{R}}^2} = -5, 5, 15, 25$ dB. Note that the

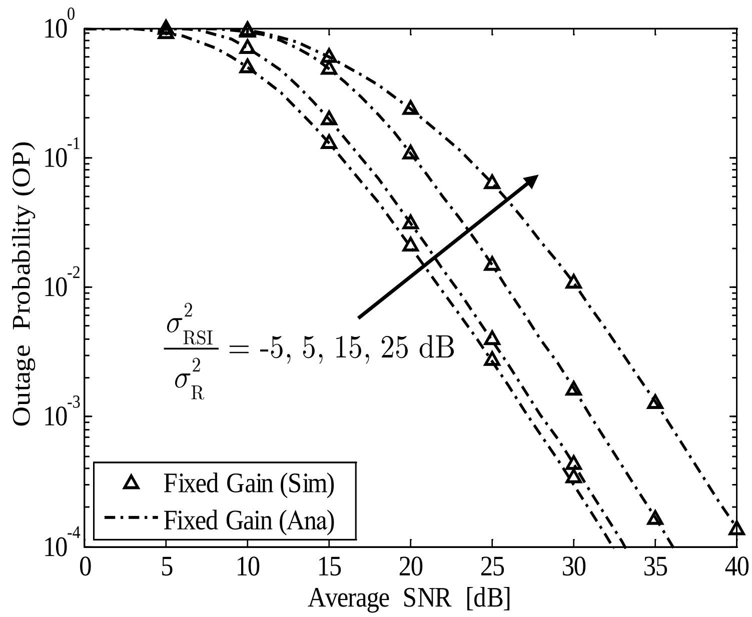

Fig. 2. The OP of the considered system in the case of fixed gain relaying versus the average SNR with fixed RSI, $\Omega_3 = 0.1$.

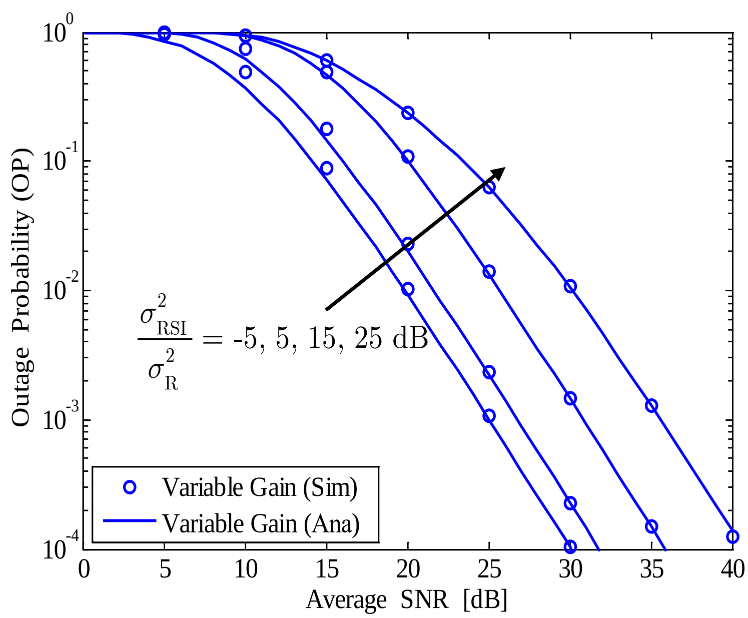

Fig. 3. The OP of the considered variable gain FD relaying system versus the average SNR for fixed RSI and different RSI power levels, $\Omega_3 = 0.1$.

RSI in this case is fixed when the transmit power at the relay node is changed. It is easy to see from these figures that since the considered system has the direct link, the outage performance is significantly improved compared with those in [37], [49], [50] where there is no direct link. Moreover, the OP does not exhibit an error floor for

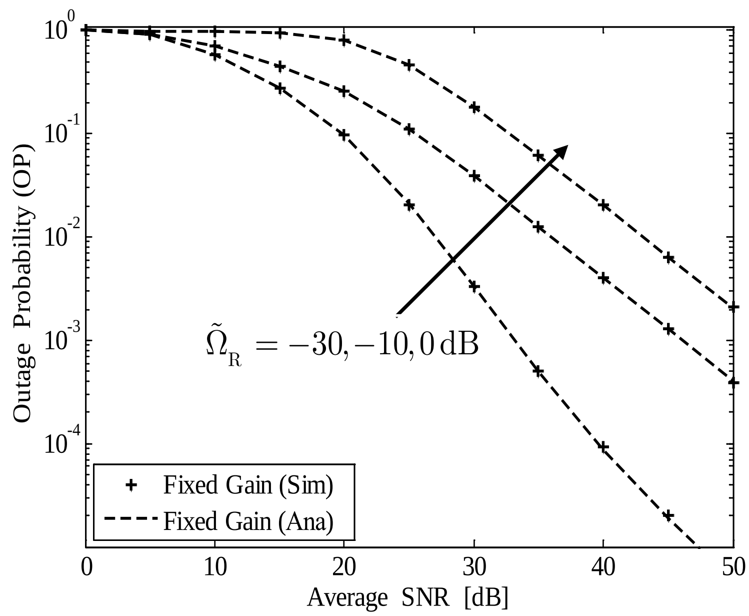

Fig. 4. The OP of the fixed gain relaying system versus the average SNR for different RSIs and without optimal power allocation, i.e. $P_{\mathrm{R}} = P_{\mathrm{S}}$.

the same settings of RSI. For example, in the case of large RSI, such as $\frac{\sigma^2_{\mathrm{RSI}}}{\sigma^2_{\mathrm{R}}} = 25$ dB, the OP of the considered system continuously reduces as the average SNR increases. It is also noted that there is a good agreement between the analytical and simulation results in the case of variable gain. For the case of fixed gain relaying, a perfect agreement can be observed. On the other hand, when RSI is small, e.g. $\frac{\sigma^2_{\mathrm{RSI}}}{\sigma^2_{\mathrm{R}}} = -5, 5$ dB, the outage performance in the case of variable gain relaying is significantly better than the fixed gain relaying case. When RSI is large enough, e.g. $\frac{\sigma^2_{\mathrm{RSI}}}{\sigma^2_{\mathrm{R}}} = 15, 25$ dB, the outage performance for the case of fixed and variable gain are similar.

Figs. 4 and 5 show the OP for the case of varied RSI for $\Omega_3 = 0.01$ and $\tilde{\Omega}_{\mathrm{R}} = -30, -10, 0$ dB. Other parameters which are used to obtain the results in the figures are similar to those in Fig. 2. It is obvious that the impact of RSI increases with the transmit power due to the following relationship $\sigma^2_{\mathrm{RSI}} = \tilde{\Omega}_{\mathrm{R}} P_{\mathrm{R}}$. Therefore, when the average SNR increases due to increasing P_{R}, σ^2_{RSI} becomes larger. We can see that when Ω_3 is very small, i.e. the direct link from S to D can be neglected, the OP will suffer an outage floor at high SNR when $P_{\mathrm{R}} = P_{\mathrm{S}}$. In order to deal with this issue, we can apply the proposed optimal power allocation. As shown in the Fig. 5, in the case of variable gain, by using the proposed optimization scheme for the FD mode, the outage performance can be significantly improved. On the other hand, when RSI is small, e.g. $\tilde{\Omega}_{\mathrm{R}} = -30$ dB, the gain difference between the cases with and without optimization are not significant. However, when RSI becomes larger, e.g $\tilde{\Omega}_{\mathrm{R}} = 0$ dB, the OP with optimization is much lower than without optimization.

Fig. 6 illustrates the system throughput of the considered system using the following settings: $\mathcal{R} = 2\,$bit/s/Hz, $\Omega_3 = 0.01$, $\tilde{\Omega}_{\mathrm{R}} = -20, -10, 0$ dB. In this figure, we use the optimal transmission power for the case with variable gain relaying. As can be seen in Fig. 6, the system throughput reaches the target $\mathcal{R}$ in the high SNR regime, such as

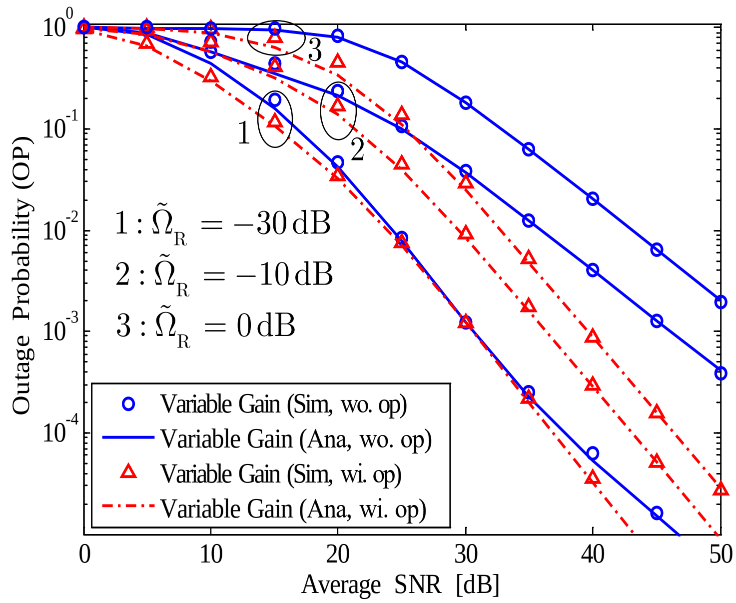

Fig. 5. The OP of the variable gain relaying system versus the average SNR for different RSIs and with/without power allocation.

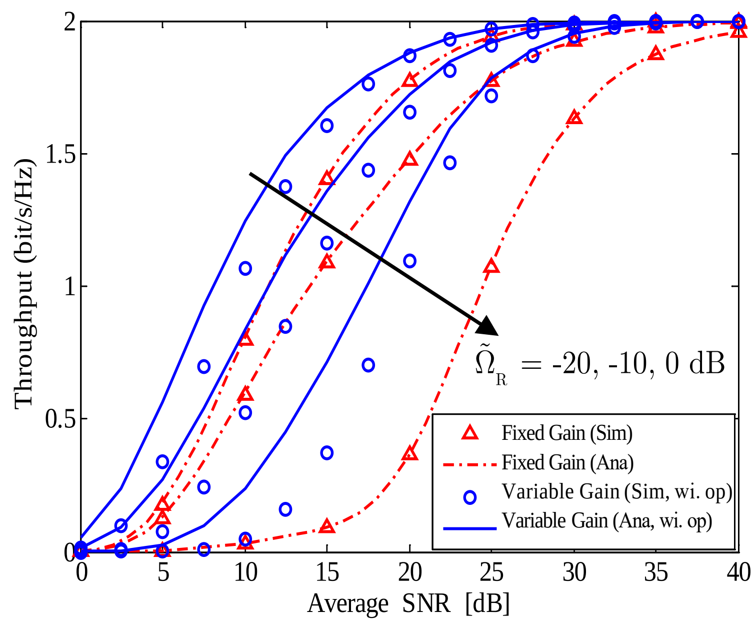

Fig. 6. The system throughput of the variable gain FD relaying system versus the average SNR at the relay node for the case using optimal power allocation and different RSIs, $\mathcal{R} = 2$, $\Omega_3 = 0.01$.

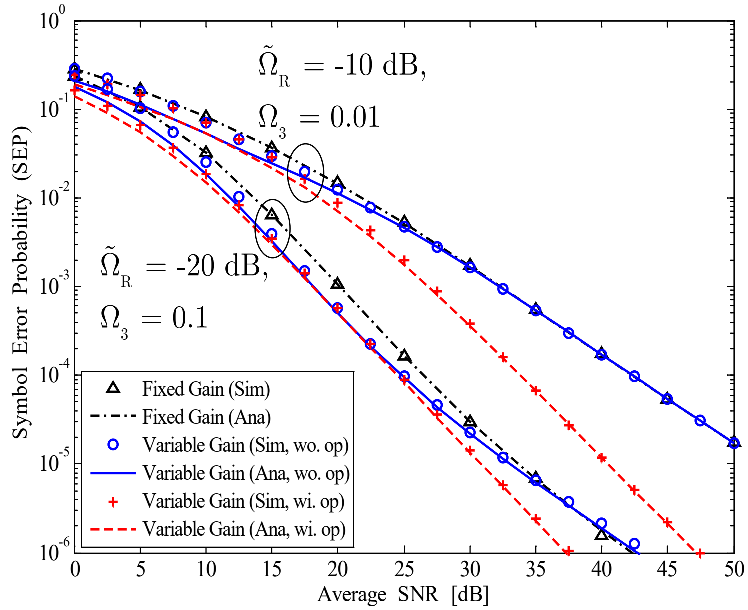

Fig. 7. The SEP of the considered fixed/variable gain FD relaying system versus the average SNR at the relay node with/without power allocation for different direct link gains and RSIs.

SNR ≈ 25 dB in the case of $\tilde{\Omega}_{\rm R} = -20$ dB, $\Omega_3 = 0.01$. When the RSI becomes larger, i.e. $\tilde{\Omega}_{\rm R} = -10, 0$ dB, the considered system achieves the target throughput with higher SNR (higher than 25 dB). Additionally, the system throughput of the case with variable gain is significantly improved in comparison with the fixed gain case when the relay power optimization is used, providing the benefit of the proposed optimal power calculation algorithm.

Fig. 7 shows the SEP of the considered system versus the average SNR at the relay when BPSK modulation ($\alpha = 1, \beta = 2$) and power allocation are used. The analytical SEP is obtained using (24) for the case of fixed gain and (25) for the case of variable gain. We investigate two cases for the direct link channel gain and the RSI, i.e. $\tilde{\Omega}_{\rm R} = -20$ dB, $\Omega_3 = 0.1$ and $\tilde{\Omega}_{\rm R} = -10$ dB, $\Omega_3 = 0.01$. Moreover, the SEP with optimal power allocation ($P_{\rm R}$ is determined by (34)) is compared with that of the case without optimal power allocation ($P_{\rm R} = P_{\rm S}$) to prove the advantage of the proposed optimal power calculation algorithm, especially in the high SNR regime. As observed from Fig. 7, when the SEP target is 10^{-4} for $\tilde{\Omega}_{\rm R} = -10$ dB, $\Omega_3 = 0.01$, the SEP with optimal power allocation has a gain of approximate 12.5 dB compared with the case of without optimal power. For the case $\tilde{\Omega}_{\rm R} = -20$ dB, $\Omega_3 = 0.1$, the gain is about 5 dB when SEP = 10^{-6}. In other word, when the channel gain of the direct link is very small, the gain in the case of optimal power becomes larger than that with higher direct link channel gain. Thanks to the proposed power allocation at the relay node, the SEP of the considered system is significantly improved. Furthermore, in the case without optimization the SEP of the fixed and variable gain relaying are similar in high SNR regime. Therefore, based on the realistic scenarios and the requirements of the FD system, RSI, and the average gain of the direct link, researchers and designers can select an appropriate transmit power of the relay node

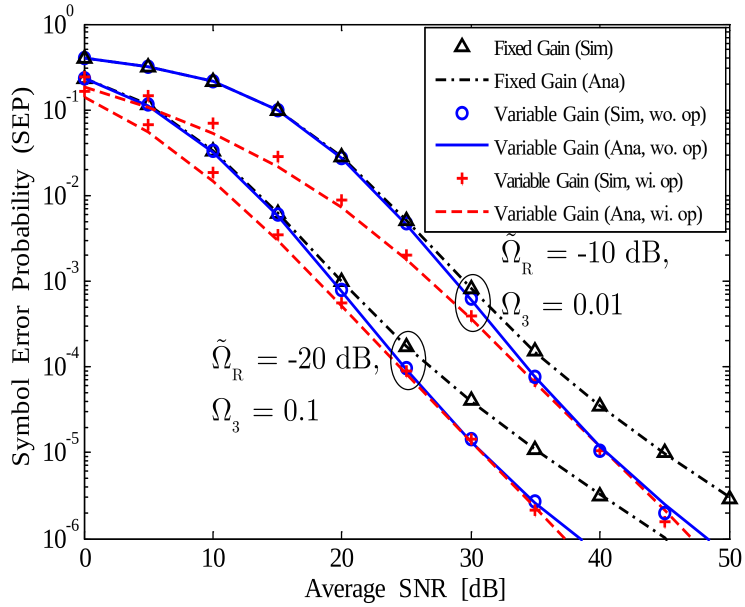

Fig. 8. The SEP of the considered fixed/variable gain FD relaying system versus the average $\mathrm{SNR} = P_{\mathrm{S}}/\sigma_{\mathrm{R}}^2$ for different channel gains and RSIs. The transmission power of the relay node is fixed so that $P_{\mathrm{R}}/\sigma_{\mathrm{D}}^2 = 25$ dB.

to improve the system performance. For example, when transmit power is large enough and the RSI level is high, to reduce the processing complexity at the relay node, we can use the fixed gain relaying to achieve the same system performance as in the case of variable gain relaying.

Fig. 8 plots the SEP in the case of relay fixed transmit power so that $P_{\mathrm{R}}/\sigma_{\mathrm{D}}^2 = 25$ dB. Other parameters are similar to those in Fig. 7. We can see that when $\mathrm{SNR} < 30$ dB the SEP for both fixed gain and variable gain in Fig. 8 is worse than that in Fig. 7. However, when $\mathrm{SNR} > 30$ dB, the SEP in Fig. 8 is better. On the other hand, for the variable gain relaying, the gain in the case with optimal power slightly increases compared with the case without optimal power. Therefore, when the FD system is affected by stronger RSI, it is important that the transmit power of the relay node is suitably selected to achieve better SEP and energy saving.

Fig. 9 presents the ergodic capacity of the system in the case of variable gain versus the average SNR at the relay node with optimal power allocation and $\tilde{\Omega}_{\mathrm{R}} = -10$ dB. In Fig. 9, the analytical curves are plotted by using (30) while the markers represent the Monte-Carlo simulation results. To consider the impact of the direct link on the system capacity, the channel gain of the direct link is varied as $\Omega_3 = 0.8, 0.5, 0.1, 0.01$. As shown in Fig. 9, the ergodic capacity improves when the SNR increases. Furthermore, increasing the channel gain of the direct link will enhance the ergodic capacity of the considered system.

VI. Conclusion

To exploit the advantages of the FD and cooperative communication systems, in this paper we have studied the performance of the AF FD relay system in the case of imperfect SIC for both fixed and variable-gain relaying.

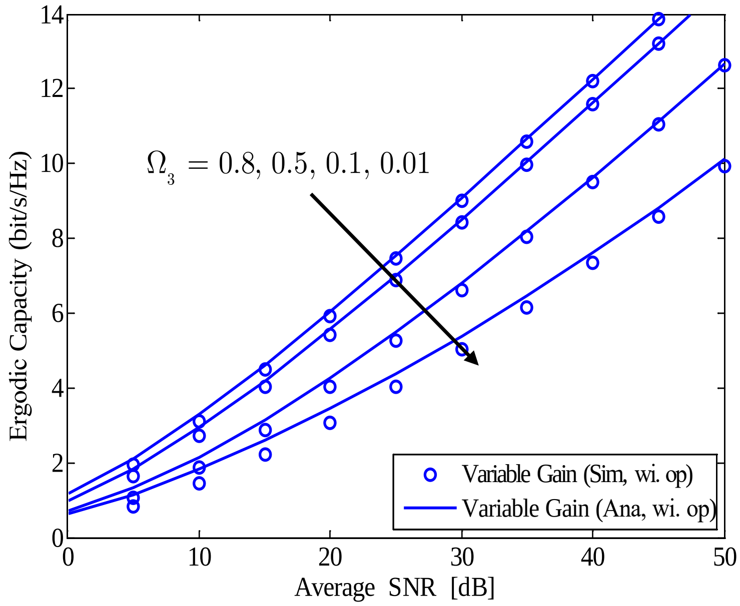

Fig. 9. The ergodic capacity of the variable gain relaying system versus the average SNR at the relay node using optimal power allocation, $\tilde{\Omega}_{\mathrm{R}} = -10$ dB.

Using theoretical analysis, we successfully derived the closed-form expressions for the OP, system throughput, ergodic capacity and SEP of the considered system. We also investigated the system performance for the case of fixed RSI and varied RSI. To improve the system performance in the case of imperfect SIC, we proposed an optimal power allocation scheme at the FD relay node. Numerical and simulation results show that the system performance is significantly improved when using the proposed power allocation scheme. When the relay cannot estimate the optimal power value to reduce the processing complexity, by using the results in this paper it is possible to select a suitable transmit power which can improve the system performance and save more energy. The results in this paper can also be easily applied to the system without direct link by setting the channel gain of this link equals zero.

APPENDIX A

This appendix provides detailed proof of Theorem 1.

1) In the case of fixed gain, we have

$$
\begin{aligned}
P_{\text{out}}^{\text{f}}(x) &= \Pr\{\gamma_{\text{SD}} + \gamma_{\text{SRD}}^{\text{f}} < x\} \\
&= \Pr\left\{\frac{\rho_3 P_{\text{S}}}{\sigma_{\text{D}}^2} + \frac{\rho_1\rho_2 P_{\text{S}}}{\rho_2(\sigma_{\text{RSI}}^2 + \sigma_{\text{R}}^2) + \sigma_{\text{D}}^2/G_{\text{f}}^2} < x\right\} \\
&= \Pr\left\{\rho_1 < \frac{\left[\rho_2(\sigma_{\text{RSI}}^2 + \sigma_{\text{R}}^2) + \sigma_{\text{D}}^2/G_{\text{f}}^2\right](x - \frac{\rho_3 P_{\text{S}}}{\sigma_{\text{D}}^2})}{\rho_2 P_{\text{S}}}\right\} \\
&= \int\limits_0^{\frac{\sigma_{\text{D}}^2 x}{P_{\text{S}}}} \left[\int_0^\infty F_{\rho_1}\left(\frac{\left[\rho_2(\sigma_{\text{RSI}}^2 + \sigma_{\text{R}}^2) + \sigma_{\text{D}}^2/G_{\text{f}}^2\right](x - \frac{\rho_3 P_{\text{S}}}{\sigma_{\text{D}}^2})}{\rho_2 P_{\text{S}}}\right)\right. \\
&\quad \left.\times f_{\rho_2}(\rho_2) d\rho_2\right] f_{\rho_3}(\rho_3) d\rho_3. \qquad (37)
\end{aligned}
$$

Applying (13) for $F_{\rho_1}(.)$ and (14) for $f_{\rho_2}(.)$ and $f_{\rho_3}(.)$ combining with [46, Eq. 3.324.1], (37) becomes

$$
\begin{aligned}
P_{\text{out}}^{\text{f}}(x) = \int\limits_0^{\frac{\sigma_{\text{D}}^2 x}{P_{\text{S}}}} &\left[1 - \exp\left(-\frac{(\sigma_{\text{RSI}}^2 + \sigma_{\text{R}}^2)(x - \frac{\rho_3 P_{\text{S}}}{\sigma_{\text{D}}^2})}{\Omega_1 P_{\text{S}}}\right)\right. \\
&\left.\times 2\sqrt{\frac{\sigma_{\text{D}}^2(x - \frac{\rho_3 P_{\text{S}}}{\sigma_{\text{D}}^2})}{\Omega_1\Omega_2 P_{\text{S}} G_{\text{f}}^2}} K_1\left(2\sqrt{\frac{\sigma_{\text{D}}^2(x - \frac{\rho_3 P_{\text{S}}}{\sigma_{\text{D}}^2})}{\Omega_1\Omega_2 P_{\text{S}} G_{\text{f}}^2}}\right)\right] \\
&\times \frac{1}{\Omega_3}\exp\Big(-\frac{\rho_3}{\Omega_3}\Big) d\rho_3 \\
&= 1 - \exp\Big(-\frac{\sigma_{\text{D}}^2 x}{\Omega_3 P_{\text{S}}}\Big) - J = 1 - \exp(-b_{\text{f}} x) - J, \qquad (38)
\end{aligned}
$$

where

$$
\begin{aligned}
J = \frac{1}{\Omega_3}\int\limits_0^{\frac{\sigma_{\text{D}}^2 x}{P_{\text{S}}}} &\exp\left(-\frac{(\sigma_{\text{RSI}}^2 + \sigma_{\text{R}}^2)(x - \frac{\rho_3 P_{\text{S}}}{\sigma_{\text{D}}^2})}{\Omega_1 P_{\text{S}}} - \frac{\rho_3}{\Omega_3}\right) \\
\times 2&\sqrt{\frac{\sigma_{\text{D}}^2(x - \frac{\rho_3 P_{\text{S}}}{\sigma_{\text{D}}^2})}{\Omega_1\Omega_2 P_{\text{S}} G_{\text{f}}^2}} K_1\left(2\sqrt{\frac{\sigma_{\text{D}}^2(x - \frac{\rho_3 P_{\text{S}}}{\sigma_{\text{D}}^2})}{\Omega_1\Omega_2 P_{\text{S}} G_{\text{f}}^2}}\right) d\rho_3. \qquad (39)
\end{aligned}
$$

Setting $\zeta = x - \frac{\rho_3 P_{\text{S}}}{\sigma_{\text{D}}^2}$, then taking integral in (39) with respect to ζ we get

$$
\begin{aligned}
J = \frac{\sigma_{\text{D}}^2}{\Omega_3 P_{\text{S}}}\exp\Big(-\frac{\sigma_{\text{D}}^2}{\Omega_3 P_{\text{S}}}\Big)\int\limits_0^x &\exp\left[-\zeta\Big(\frac{\sigma_{\text{RSI}}^2 + \sigma_{\text{R}}^2}{\Omega_1 P_{\text{S}}} - \frac{\sigma_{\text{D}}^2}{\Omega_3 P_{\text{S}}}\Big)\right] \\
\times 2\sqrt{\frac{\sigma_{\text{D}}^2\zeta}{\Omega_1\Omega_2 P_{\text{S}} G_{\text{f}}^2}} &K_1\left(2\sqrt{\frac{\sigma_{\text{D}}^2\zeta}{\Omega_1\Omega_2 P_{\text{S}} G_{\text{f}}^2}}\right) d\zeta. \qquad (40)
\end{aligned}
$$

Applying the Gaussian-Chebyshev quadrature method [47], then (40) becomes

$$
\begin{aligned}
J &= \frac{\sigma_{\text{D}}^2 x}{2\Omega_3 P_{\text{S}}}\exp\Big(-\frac{\sigma_{\text{D}}^2 x}{\Omega_3 P_{\text{S}}}\Big)\sum_{n=1}^N \frac{\pi}{N}\sqrt{1-\phi_n^2}G(u) \\
&= \frac{b_{\text{f}} x}{2}\exp(-b_{\text{f}} x)\sum_{n=1}^N \frac{\pi}{N}\sqrt{1-\phi_n^2}G(u), \qquad (41)
\end{aligned}
$$

where $G(u)$ is given in (21).

2) In the case of variable gain, we have

$$P_{\text{out}}^{\text{v}}(x)=\Pr\left\{\frac{\rho_3 P_{\text{S}}}{\sigma_{\text{D}}^2}+\frac{\rho_1\rho_2 P_{\text{S}} P_{\text{R}}}{(\rho_2 P_{\text{R}}+\sigma_{\text{D}}^2)(\sigma_{\text{RSI}}^2+\sigma_{\text{R}}^2)+\rho_1 P_{\text{S}}\sigma_{\text{D}}^2}<x\right\} \tag{42}$$

Therefore

$$\begin{aligned}
P_{\text{out}}^{\text{v}}(x)=&\int_0^{\frac{\sigma_{\text{D}}^2 x}{P_{\text{S}}}}\left[1-\int_0^{\infty}\Big[1-F_{\rho_1}(v)\Big]f_{\rho_2}(z+\frac{\sigma_{\text{D}}^2}{P_{\text{R}}}\zeta)dz\right]f_{\rho_3}(\rho_3)d\rho_3\\
=&\int_0^{\frac{\sigma_{\text{D}}^2 x}{P_{\text{S}}}}\left[1-\exp(-a_{\text{v}}\zeta)2\sqrt{\frac{\sigma_{\text{D}}^2(\sigma_{\text{RSI}}^2+\sigma_{\text{R}}^2)(\zeta^2+\zeta)}{\Omega_1\Omega_2 P_{\text{S}} P_{\text{R}}}}\right.\\
&\left.\times K_1\left(2\sqrt{\frac{\sigma_{\text{D}}^2(\sigma_{\text{RSI}}^2+\sigma_{\text{R}}^2)(\zeta^2+\zeta)}{\Omega_1\Omega_2 P_{\text{S}} P_{\text{R}}}}\right)\right]f_{\rho_3}(\rho_3)d\rho_3\\
\approx&\int_0^{\frac{\sigma_{\text{D}}^2 x}{P_{\text{S}}}}\left[1-\exp(-a_{\text{v}}\zeta)\right]f_{\rho_3}(\rho_3)d\rho_3\\
=&\int_0^{\frac{\sigma_{\text{D}}^2 x}{P_{\text{S}}}}\left[1-\exp(-a_{\text{v}}(x-\frac{\rho_3 P_{\text{S}}}{\sigma_{\text{D}}^2}))\right]\frac{1}{\Omega_3}\exp(-\frac{\rho_3}{\Omega_3})d\rho_3,
\end{aligned} \tag{43}$$

where

$$v=\frac{\left[(z+\frac{\sigma_{\text{D}}^2}{P_{\text{R}}}\zeta)P_{\text{R}}+\sigma_{\text{D}}^2\right](\sigma_{\text{RSI}}^2+\sigma_{\text{R}}^2)\zeta}{P_{\text{S}} P_{\text{R}} z}.$$

After some mathematical transforms, we can obtain the $P_{\text{out}}^{\text{v}}(x)$ as in (20).

The proof of Theorem 1 is complete.

Appendix B

This appendix provides detailed proof of Theorem 2.

1) In the case of fixed gain, the SEP^{f} is determined as follows

$$\begin{aligned}
\text{SEP}^{\text{f}}=&\frac{\alpha\sqrt{\beta}}{2\sqrt{2\pi}}\int_0^{\infty}\frac{e^{-\beta x/2}}{\sqrt{x}}\left[1-\exp(-b_{\text{f}}x)-\frac{b_{\text{f}}x}{2}\exp(-b_{\text{f}}x)\right.\\
&\left.\times\sum_{n=1}^{N}\frac{\pi}{N}\sqrt{1-\phi_n^2}G(u)\right]dx
\end{aligned} \tag{44}$$

Applying [46, Eq. 3.361.1], the first part of the integral in (44) is given by

$$\int_0^{\infty}\frac{e^{-\beta x/2}}{\sqrt{x}}\Big[1-\exp(-b_{\text{f}}x)\Big]dx=\sqrt{\frac{2\pi}{\beta}}-\sqrt{\frac{2\pi}{\beta+2b_{\text{f}}}}. \tag{45}$$

For the second part of the integral in (44), we have

$$\int_0^{\infty} \frac{e^{-\beta x/2}}{\sqrt{x}} \frac{b_{\mathrm{f}} x}{2} \exp(-b_{\mathrm{f}} x) \sum_{n=1}^{N} \frac{\pi}{N} \sqrt{1-\phi_n^2} G\Big(\frac{x}{2}(\phi_n+1)\Big) dx$$
$$= \frac{b_{\mathrm{f}}\pi}{N} \sum_{n=1}^{N} \chi \sqrt{1-\phi_n^2} \int_0^{\infty} x \exp(-\varphi x) K_1\Big(2\chi\sqrt{x}\Big) dx, \quad (46)$$

where the parameters χ and φ are defined in (27). Using the [46, Eq. 6.643.3], the integral in (46) can be calculated as

$$\int_0^{\infty} x \exp(-\varphi x) K_1\Big(2\chi\sqrt{x}\Big) dx = \frac{\Gamma(\frac{5}{2})\Gamma(\frac{3}{2})}{2\chi} \exp\Big(\frac{\chi^2}{2\varphi}\Big)$$
$$\times \varphi^{-\frac{3}{2}} W\Big(-\frac{3}{2}, \frac{1}{2}, \frac{\chi^2}{\varphi}\Big) \quad (47)$$

After some mathematical manipulations, we obtain the $\mathrm{SEP}^{\mathrm{f}}$ of the considered system as in (24).

2) In the case of variable gain, the SEP of the considered system is determined as

$$\mathrm{SEP}^{\mathrm{v}} = \begin{cases} \frac{\alpha\sqrt{\beta}}{2\sqrt{2\pi}} \int\limits_0^{\infty} \frac{e^{-\beta x/2}}{\sqrt{x}} \Big(1 - \frac{b_{\mathrm{v}}}{b_{\mathrm{v}}-a_{\mathrm{v}}} e^{-a_{\mathrm{v}} x} - \frac{a_{\mathrm{v}}}{a_{\mathrm{v}}-b_{\mathrm{v}}} e^{-b_{\mathrm{v}} x}\Big) dx, & a_{\mathrm{v}} \neq b_{\mathrm{v}} \\ \frac{\alpha\sqrt{\beta}}{2\sqrt{2\pi}} \int\limits_0^{\infty} \frac{e^{-\beta x/2}}{\sqrt{x}} \Big(1 - b_{\mathrm{v}} x e^{-a_{\mathrm{v}} x} - e^{-b_{\mathrm{v}} x}\Big) dx, & a = b \end{cases}$$
$$= \begin{cases} \frac{\alpha\sqrt{\beta}}{2\sqrt{2\pi}} \Big(\sqrt{\frac{2\pi}{\beta}} - \frac{b_{\mathrm{v}}}{b_{\mathrm{v}}-a_{\mathrm{v}}} \sqrt{\frac{2\pi}{\beta+2a_{\mathrm{v}}}} - \frac{a_{\mathrm{v}}}{a_{\mathrm{v}}-b_{\mathrm{v}}} \sqrt{\frac{2\pi}{\beta+2b_{\mathrm{v}}}}\Big), & a_{\mathrm{v}} \neq b_{\mathrm{v}} \\ \frac{\alpha\sqrt{\beta}}{2\sqrt{2\pi}} \Big(\sqrt{\frac{2\pi}{\beta}} - \sqrt{\frac{2\pi}{\beta+2b_{\mathrm{v}}}} - b_{\mathrm{v}} \sqrt{\frac{2\pi}{(\beta+2a_{\mathrm{v}})^3}}\Big), & a_{\mathrm{v}} = b_{\mathrm{v}}. \end{cases} \quad (48)$$

It is noted that the first line in (48) is obtained by using [46, Eq. 3.361.1] while the second line is obtained by using both [46, Eq. 2.321.1 and Eq. 3.361.1]. After some mathematical transforms, we have the $\mathrm{SEP}^{\mathrm{v}}$ as in (25). The proof of Theorem 2 is complete.

References

[1] B. C. Nguyen, X. N. Tran, and D. T. Tran, "Performance analysis of in-band full-duplex amplify-and-forward relay system with direct link," in *2nd International Conference on Recent Advances in Signal Processing, Telecommunications Computing (SigTelCom)*, Jan 2018, pp. 192–197.

[2] Q. C. Li, H. Niu, A. T. Papathanassiou, and G. Wu, "5g network capacity: Key elements and technologies," *IEEE Vehicular Technology Magazine*, vol. 9, no. 1, pp. 71–78, 2014.

[3] S. Hong, J. Brand, J. I. Choi, M. Jain, J. Mehlman, S. Katti, and P. Levis, "Applications of self-interference cancellation in 5G and beyond," *IEEE Commun. Mag.*, vol. 52, no. 2, pp. 114–121, Feb. 2014.

[4] F.-L. Luo and C. Zhang, *Signal processing for 5G: algorithms and implementations*. John Wiley & Sons, 2016.

[5] X. N. Tran, B. C. Nguyen, and D. T. Tran, "Outage probability of two-way full-duplex relay system with hardware impairments," in *3rd International Conference on Recent Advances in Signal Processing, Telecommunications & Computing (SigTelCom)*. IEEE, 2019, pp. 135–139.

[6] Z. Kaleem, N. N. Qadri, T. Q. Duong, and G. K. Karagiannidis, "Energy-efficient device discovery in d2d cellular networks for public safety scenario," *IEEE Systems Journal*, 2019.

[7] Z. Uddin, A. Ahmad, M. Iqbal, and Z. Kaleem, "Adaptive step size gradient ascent ica algorithm for wireless mimo systems," *Mobile Information Systems*, vol. 2018, 2018.

[8] N.-P. Nguyen, H. Q. Ngo, T. Q. Duong, H. D. Tuan, and D. B. da Costa, "Full-duplex cyber-weapon with massive arrays," *IEEE Transactions on Communications*, vol. 65, no. 12, pp. 5544–5558, 2017.

[9] H. H. M. Tam, H. D. Tuan, A. A. Nasir, T. Q. Duong, and H. V. Poor, "Mimo energy harvesting in full-duplex multi-user networks," *IEEE Transactions on Wireless Communications*, vol. 16, no. 5, pp. 3282–3297, 2017.

[10] V.-D. Nguyen, T. Q. Duong, H. D. Tuan, O.-S. Shin, and H. V. Poor, "Spectral and energy efficiencies in full-duplex wireless information and power transfer," *IEEE Transactions on Communications*, vol. 65, no. 5, pp. 2220–2233, 2017.

[11] T. Zhang, Y. Cai, Y. Huang, T. Q. Duong, and W. Yang, "Secure full-duplex spectrum-sharing wiretap networks with different antenna reception schemes," *IEEE Transactions on Communications*, vol. 65, no. 1, pp. 335–346, 2016.

[12] Y. Deng, K. J. Kim, T. Q. Duong, M. Elkashlan, G. K. Karagiannidis, and A. Nallanathan, "Full-duplex spectrum sharing in cooperative single carrier systems," *IEEE Transactions on Cognitive Communications and Networking*, vol. 2, no. 1, pp. 68–82, 2016.

[13] N.-P. Nguyen, C. Kundu, H. Q. Ngo, T. Q. Duong, and B. Canberk, "Secure full-duplex small-cell networks in a spectrum sharing environment," *IEEE Access*, vol. 4, pp. 3087–3099, 2016.

[14] X.-T. Doan, N.-P. Nguyen, C. Yin, D. B. Da Costa, and T. Q. Duong, "Cognitive full-duplex relay networks under the peak interference power constraint of multiple primary users," *EURASIP Journal on Wireless Communications and Networking*, vol. 2017, no. 1, p. 8, 2017.

[15] B. C. Nguyen, T. M. Hoang, and P. T. Tran, "Performance analysis of full-duplex decode-and-forward relay system with energy harvesting over nakagami-m fading channels," *AEU-International Journal of Electronics and Communications*, vol. 98, pp. 114–122, 2019.

[16] A. Sabharwal, P. Schniter, D. Guo, D. W. Bliss, S. Rangarajan, and R. Wichman, "In-band full-duplex wireless: Challenges and opportunities," *IEEE J. Sel. Areas in Commun.*, vol. 32, no. 9, pp. 1637–1652, 2014.

[17] K. Yang, H. Cui, L. Song, and Y. Li, "Efficient full-duplex relaying with joint antenna-relay selection and self-interference suppression," *IEEE Trans. Wireless Commun.*, vol. 14, no. 7, pp. 3991–4005, Jul. 2015.

[18] E. Ahmed, A. M. Eltawil, and A. Sabharwal, "Self-interference cancellation with nonlinear distortion suppression for full-duplex systems," in *Signals, Systems and Computers, Asilomar Conference on*. IEEE, 2013, pp. 1199–1203.

[19] E. Ahmed and A. M. Eltawil, "All-digital self-interference cancellation technique for full-duplex systems," *IEEE Transactions on Wireless Communications*, vol. 14, no. 7, pp. 3519–3532, 2015.

[20] E. Antonio-Rodrguez, R. Lpez-Valcarce, T. Riihonen, S. Werner, and R. Wichman, "Adaptive self-interference cancellation in wideband full-duplex decode-and-forward mimo relays," in *Signal Processing Advances in Wireless Communications (SPAWC), IEEE 14th Workshop on*. IEEE, 2013, pp. 370–374.

[21] D. Bharadia, E. McMilin, and S. Katti, "Full duplex radios," in *ACM SIGCOMM Computer Communication Review*, vol. 43. ACM, 2013, Conference Proceedings, pp. 375–386.

[22] C. Yin, H. T. Nguyen, C. Kundu, Z. Kaleem, E. Garcia-Palacios, and T. Q. Duong, "Secure energy harvesting relay networks with unreliable backhaul connections," *IEEE Access*, vol. 6, pp. 12 074–12 084, 2018.

[23] A. H. Gazestani, S. A. Ghorashi, B. Mousavinasab, and M. Shikh-Bahaei, "A survey on implementation and applications of full duplex wireless communications," *Physical Communication*, 2019.

[24] Z. Kaleem, M. Yousaf, S. A. Hassan, N.-S. Vo, and T. Q. Duong, "Priority-based device discovery in public safety d2d networks with full duplexing," in *International Conference on Heterogeneous Networking for Quality, Reliability, Security and Robustness*. Springer, 2018, pp. 102–108.

[25] Z. Kaleem, A. Khan, S. A. Hassan, N.-S. Vo, L. D. Nguyen, and H. M. Nguyen, "Full-duplex enabled time-efficient device discovery for public safety communications," *Mobile Networks and Applications*, pp. 1–9, 2019.

[26] B. C. Nguyen, X. N. Tran, T. M. Hoang *et al.*, "Performance analysis of full-duplex vehicle-to-vehicle relay system over double-rayleigh fading channels," *Mobile Networks and Applications*, pp. 1–10, 2019.

[27] B. C. Nguyen and X. N. Tran, "Performance analysis of full-duplex amplify-and-forward relay system with hardware impairments and imperfect self-interference cancellation," *Wireless Communications and Mobile Computing*, vol. 2019, p. 10, 2019.

[28] D. P. M. Osorio, E. E. B. Olivo, H. Alves, J. C. S. S. Filho, and M. Latva-aho, "Exploiting the direct link in full-duplex amplify-and-forward relaying networks," *IEEE Signal Process. Lett.*, vol. 22, no. 10, pp. 1766–1770, Oct. 2015.

[29] K. C. Dheeraj, A. Thangaraj, and R. Ganti, "Equalization in amplify-forward full-duplex relay with direct link," in *Proc. 21st Nat. Conf. Commun. (NCC)*, Feb. 2015, pp. 1–6.

[30] T. M. Hoang, V. Van Son, N. C. Dinh, and P. T. Hiep, "Optimizing duration of energy harvesting for downlink noma full-duplex over nakagami-m fading channel," *AEU-International Journal of Electronics and Communications*, vol. 95, pp. 199–206, 2018.

[31] G. Liu, W. Feng, Z. Han, and W. Jiang, "Performance analysis and optimization of cooperative full-duplex d2d communication underlaying cellular networks," *arXiv preprint arXiv:1805.06645*, 2018.

[32] D. Zhang, Y. Liu, L. Dai, A. K. Bashir, A. Nallanathan, and B. Shim, "Performance analysis of fd-noma-based decentralized v2x systems," *IEEE Transactions on Communications*, 2019.

[33] O. Abbasi and A. Ebrahimi, "Cooperative noma with full-duplex amplify-and-forward relaying," *Transactions on Emerging Telecommunications Technologies*, vol. 29, no. 7, p. e3421, 2018.

[34] B. Li, X. Qi, K. Huang, Z. Fei, F. Zhou, and R. Q. Hu, "Security-reliability tradeoff analysis for cooperative noma in cognitive radio networks," *IEEE Transactions on Communications*, vol. 67, no. 1, pp. 83–96, 2019.

[35] S. Wang and T. Wu, "Stochastic geometric performance analyses for the cooperative noma with the full-duplex energy harvesting relaying," *IEEE Transactions on Vehicular Technology*, pp. 1–1, 2019.

[36] T. Riihonen, S. Werner, and R. Wichman, "Hybrid full-duplex/half-duplex relaying with transmit power adaptation," *IEEE Trans. Wireless Commun.*, vol. 10, no. 9, pp. 3074–3085, Sept. 2011.

[37] T. M. Kim and A. Paulraj, "Outage probability of amplify-and-forward cooperation with full duplex relay," in *Proc. IEEE Wireless Commun. Netw. Conf (WCNC)*, Apr. 2012, pp. 75–79.

[38] P. L. Yeoh, M. Elkashlan, and I. B. Collings, "Selection relaying with transmit beamforming: A comparison of fixed and variable gain relaying," *IEEE Transactions on Communications*, vol. 59, no. 6, pp. 1720–1730, 2011.

[39] X. Yue, Y. Liu, S. Kang, A. Nallanathan, and Z. Ding, "Exploiting full/half-duplex user relaying in noma systems," *IEEE Transactions on Communications*, vol. 66, no. 2, pp. 560–575, Feb 2018.

[40] Z. Zhang, Z. Ma, M. Xiao, Z. Ding, and P. Fan, "Full-duplex device-to-device-aided cooperative nonorthogonal multiple access," *IEEE Transactions on Vehicular Technology*, vol. 66, no. 5, pp. 4467–4471, May 2017.

[41] B. C. Nguyen, T. M. Hoang, S.-G. Choi *et al.*, "Full-duplex relay system with energy harvesting: Outage and symbol error probabilities," in *International Conference on Advanced Technologies for Communications (ATC)*. IEEE, 2018, pp. 360–365.

[42] X. Li, C. Tepedelenlioglu, and H. Senol, "Channel estimation for residual self-interference in full duplex amplify-and-forward two-way relays," *IEEE Trans. Wireless Commun.*, vol. PP, no. 99, pp. 1–1, 2017.

[43] T. M. Hoang, N. T. Tan, N. B. Cao *et al.*, "Outage probability of mimo relaying full-duplex system with wireless information and power transfer," in *Conference on Information and Communication Technology (CICT)*. IEEE, 2017, pp. 1–6.

[44] B. C. Nguyen, T. M. Hoang *et al.*, "Performance analysis of vehicle-to-vehicle communication with full-duplex amplify-and-forward relay over double-rayleigh fading channels," *Vehicular Communications*, vol. 19, p. 100166, 2019.

[45] X. Yue, Y. Liu, S. Kang, A. Nallanathan, and Z. Ding, "Exploiting full/half-duplex user relaying in noma systems," *IEEE Transactions on Communications*, vol. PP, no. 99, pp. 1–1, 2017.

[46] A. Jeffrey and D. Zwillinger, *Table of integrals, series, and products*. Academic press, 2007.

[47] M. Abramowitz and I. A. Stegun, *Handbook of mathematical functions with formulas, graphs, and mathematical tables*. Dover, New York, 1972, vol. 9.

[48] A. Goldsmith, *Wireless communications*. Cambridge university press, 2005.

[49] I. Krikidis, H. A. Suraweera, P. J. Smith, and C. Yuen, "Full-duplex relay selection for amplify-and-forward cooperative networks," *IEEE Trans. Wireless Commun.*, vol. 11, no. 12, pp. 4381–4393, 2012.

[50] S. Li, Y. Kun, M. Zhou, J. Wu, L. Song, Y. Li, and H. Li, "Full-duplex amplify-and-forward relaying: Power and location optimization," *IEEE Trans. Veh. Technol.*, vol. PP, no. 99, pp. 1–1, 2017.